Int. J. Heat Mass Transfer. Vol. 31, No. 8, pp. 1701–1710, 1988
Printed in Great Britain

0017-9310/88 $3.00+0.00

Thermal instability in gently heated unsaturated sand

JOHN EWEN
Solar Energy Unit, Department of Mechanical Engineering and Energy Studies,
University College, Newport Road, Cardiff CF2 1TA, U.K.

(*Received* 4 *December* 1987 *and in final form* 9 *February* 1988)

Abstract—Samples of unsaturated sand were heated a few tens of Kelvin by a small cylindrical heater. The radial temperature profiles presented in this paper clearly show instability as a dry region develops around the heater. A simple and generally useful empirical model with three constant parameters is developed. Two of the parameters are the effective thermal conductivities in the dry and moist sand while the third relates to the rate of drying.

INTRODUCTION

IF THE low-grade thermal energy in hot water from solar thermal collector arrays and industrial process equipment is to be exploited it must be transported and stored cheaply: the energy has a small economic value as its low intensity makes it expensive to transfer from one material to another or to convert to work. For schemes of a medium to large scale, buried pipelines and ground based reservoirs are appropriate means of transportation and storage. Unfortunately, these devices usually need to be surrounded by bulky and relatively expensive thermal insulation.

Experiments conducted for the electricity supply industry [1] have shown that when unsaturated uniformly graded soil is subjected to a sustained thermal gradient it dries out and its effective thermal conductivity falls to a low value. This suggests that uniformly graded sand used as backfill around hot buried pipelines or ground based thermal reservoirs will act as a natural and robust thermal insulating material. If successful the sand will have two advantages over other insulating materials: it is cheap and easily handled.

Two studies of the performance of a particular sand have been completed. In the first study full sets of data for the porosity, capillary potential, unsaturated hydraulic conductivity and thermal conductivity of the sand were collected from a series of laboratory experiments. Analytic expressions representing these data as functions of the sand's dry density, moisture content and temperature were then incorporated in numerical finite difference models describing combined heat and mass transfer. The major part of this work has been reported elsewhere [2] and a report on a model describing combined heat and mass transfer in a two-dimensional space, including gravitational effects, is being prepared.

The subject of this paper is the second study. In this the simplest possible empirical model was sought; it was found that only three constant parameters are required to describe the thermal response of the sand when used as a backfill around a buried pipeline. The values of the parameters are easily identifiable and there is evidence that their variation with soil condition is predictable.

To satisfy the original aim of the study, the empirical model may be applied directly to predict the long-term performance of the sand when used as a backfill. However, because it is both simple and accurate, the empirical model has more general uses. It may, for example, be used to identify the significant terms in detailed models of combined heat and mass transfer. Numerical models containing only these terms may then be used to predict thermally unstable behaviour in regions with complex geometry or where gravitational influences are not negligible.

A promising use for the empirical model is in the choice of backfill material. If the empirical model is applicable to other thermally unstable soils, the values of the three parameters identified for any soil will characterize its thermal insulating properties. The properties of a range of different soils may then be compared and the best backfill identified.

The experimental method, the development of the empirical model and the identification of the three parameters are described in this paper. A few conclusions are then drawn from the form of the empirical model.

EXPERIMENTAL DESIGN AND EQUIPMENT

The sand studied is sold under the trade name Garside Grade 21. It is a uniformly graded medium sand sieved from Leighton Buzzard Lower Green sand; by mass it is over 96% quartz. The particle size distribution for the sand is given in Table 1; other properties are listed in the Appendix. All samples tested were compacted to a dry density of 1580 kg m^{-3}. The corresponding porosity has been calculated as 0.41 by volume on the assumption that the density of the individual grains is 2700 kg m^{-3}.

NOMENCLATURE

a	radius of cylindrical heater [m]
D	drying diffusivity [$m^2 s^{-1}$]
$\hat{D}$	drying constant [$m^3 J^{-1}$]
f	arbitrary function of time
g	gravitational constant [$m s^{-2}$]
h	arbitrary function of heating power
k	effective thermal conductivity [$W m^{-1} K^{-1}$]
k_d	effective thermal conductivity in the dry region [$W m^{-1} K^{-1}$]
k_m	effective thermal conductivity in the moist region [$W m^{-1} K^{-1}$]
K	unsaturated hydraulic conductivity [s]
L	latent heat of vaporization for soil water [$J kg^{-1}$]
M	volumetric moisture content in the moist region [—]
q	mass flow rate with the dry/moist front [$kg s^{-1} m^{-1}$]
Q	heating power supplied to heater [$W m^{-1}$]
r	radius [m]
s	radius of the dry/moist front [m]
S	degree of saturation [—]
t	time [s]
T	temperature [K]
W	predicted temperature [K]
Z	length scale defined in equation (3) for heating at constant power [—] and defined in equation (12) for heating at constant temperature [$W m^{-1}$]
Z'	value of length scale Z at the dry/moist front.

Greek symbols

α	empirical constant [—]
Γ	empirical constant defined in equation (6) [—]
Λ	empirical constant defined in equation (7) for heating at constant power [K] and defined in equation (13) for heating at constant temperature [$m K W^{-1}$]
ρ	density of liquid soil water [$kg m^{-3}$]
ψ	capillary potential [$J kg^{-1}$].

Table 1. Particle size distribution

Mesh size (mm)	Percentage passing
1.18	100
0.60	86
0.425	27
0.300	12
0.212	4
0.150	1
0.063	0

Fortunately, the condition of sand newly compacted around buried pipelines can be easily and accurately recreated in the laboratory; the thermal behaviour under field conditions can therefore be studied using a bench-top heating experiment.

The design of a suitable experiment was influenced by the published experience of several investigators. In 1943, Smith [3] reported measuring the moisture content variation induced across thin slabs of soil subjected to a thermal gradient. To obtain his data he took sub-samples and determined their moisture content by measuring the difference in mass of the sub-samples before and after drying at 105°C for 24 h. No better method is yet available for the determination of the moisture distribution in heated samples; in 1981 Baladi *et al.* [4] reported on the use of specially designed electric capacitance moisture probes and concluded they were too large and have too slow a transient response to be of practical use.

The most common geometry for samples is a cylinder. In 1954, Rollins *et al.* [5] described tests performed on 100 mm long, 50 mm diameter samples in which thermal gradients were induced along the axes of generation of the cylinders. Shah *et al.* [6] tested samples 150 and 300 mm long but only 35 mm in diameter; in 1984 they published plots of steady moisture distribution as well as plots of steady temperature measured at the sites of thermocouples distributed along the length of the samples.

The main drawback with the axial heating of cylindrical samples seems to be that radial heat losses cannot easily be eliminated. Shah *et al.* [6] insulated their samples and surrounded the insulation with a guard heater. It is not reported how effective this approach was. In 1986 Couvillion and Hartley [7] described experiments in which (despite heavily insulating the sample) radial heat losses were significant to the extent that they were specifically studied. During the validation of a numerical computer model of combined heat and mass transfer in soil it was attempted to eliminate the influence of the radial heat losses by modelling them using a fin-type heat transfer analysis.

In more robust experiments, power is supplied to a spherical or cylindrical heater embedded in a sample of soil. Baladi *et al.* [4] reported burying a 40 mm diameter spherical heater in a large cylindrical sample of soil (920 mm in diameter by 920 mm long). To accurately record the high temperature gradient expected near the sphere they did not distribute thermocouples evenly with radius but positioned those nearest the heater closer together. Two sets of thermocouples were installed and two-dimensional tem-

perature effects were recorded; temperatures in the horizontal plane of the heater were higher than those below and in the vertical plane of the heater.

In 1968 Adams and Baljet [1] described experiments in which a 102 mm long 25.4 mm diameter cylindrical heater was positioned in 150 mm long by 150 mm diameter cylindrical samples. The plane ends of the samples were heavily insulated but the steel sample cylinder was not; heat travelled from the heater, through the sample, passed through the steel cylinder wall, and into the surrounding air.

In the experiments described here this robust approach is adopted. A cylindrical heater is buried in a cylindrical sample of sand. To minimize axial temperature variations the heater runs the full length of the sample, from one insulated plane end to the other. Power is supplied to the heater and the resulting temperature rise in the sample is recorded using thermocouples distributed along radials above, horizontal in line with, and below the heater; along each radial, individual thermocouples are distributed at approximately equal intervals of the logarithm of radius. By this approach two-dimensional gravitational effects can be isolated and good estimates can be obtained for the radial temperature gradient.

Under steady or quasi-steady conditions the estimates of radial temperature gradient can be used to obtain estimates of the local effective thermal conductivity: from Fourier's law of heat conduction, at any radius r subject to radial heat flux Q, the radial temperature gradient is given by

$$\frac{\partial T}{\partial \ln r} = \frac{Q}{2\pi k} \tag{1}$$

where T is temperature and k the local effective thermal conductivity.

At the end of an experiment the sample can be examined and the steady moisture content distribution determined by taking and testing subsamples. Unfortunately, as discussed earlier, no successful experimental method has yet been reported for monitoring moisture redistribution during heating. However, on examining a sample of sand during a field test, Adams and Baljet [1] found that dried sand could be distinguished from moist sand by its light colour. Couvillion and Hartley [7] monitored this colour change through an axially heated sample and called the boundary between the light and dark soil the dry/moist front. As the progress of the dry/moist front cannot be monitored visually in a radially heated sample, an indirect method has been developed to determine the progress of the dry/moist front. This method is described later.

Experimental rig

The heater and the container for the sand samples are shown in Fig. 1. An electric resistance wire lies within the 525 mm long, 12.7 mm diameter, 16 gauge aluminium tube that forms the heater body. Heating is effected by supplying electric current to the wire from a standard stabilized laboratory power supply. The heater is kept in place by being squeezed between the top and bottom end-pieces which hold the sample within the sample container. The end-pieces are thermally insulated by 25 mm compressed fibre insulating board glued to their outer surfaces. The sample container is glass with internal length 522 mm and diameter 219.6 mm giving it a capacity of 0.0198 m^3.

There are two feed-through fittings in the top end-piece: a central fitting for the heater supply cable and a bottom fitting for the instrumentation (thermocouple) wires. Twenty-four nickel–chromium/nickel–aluminium thermocouples enter through the bottom fitting as three groups of eight. Each group is fixed on a nylon former designed to lie radially and fit firmly between the heater and the wall of the glass sample container. The individual thermocouples were positioned on the formers such that they lie at fixed radial distances from the centre of the heater: 7.9, 11.4, 16.4, 26.4, 41.4, 56.4, 86.4 and 103.9 mm.

The 24 thermocouples were calibrated along with five others. All were attached to a 30-way manual thermocouple digital-read-out-box and placed in a constant temperature water bath alongside a standard mercury-in-glass thermometer. The combined accuracy of the thermocouples and the digital-read-out-box was found to be ± 0.25 K in the range 20–95°C. The precision of the thermocouples as a group was ± 0.2 K: when tested simultaneously the temperatures recorded for all 29 thermocouples were within ± 0.2 K.

Before each sample was loaded, the sample container was marked-off into six equal volumes, the bottom end-piece and the heater were fitted, and the assembly positioned with the bottom end-piece flat on the floor. Three charges of sand were then loaded. Each was weighed, wetted by a measured mass of de-aired distilled water, mixed for 3 min in a bakery type mechanical mixer and tamped into a marked section of the sample container. At this point the three nylon formers were laid on top of the sample. One former was fitted tightly between the heater and the wall of the sample container; the others were similarly fitted to lie at 90° and 180° to the first. The final three charges of sand were then prepared and loaded and the top end-piece fitted.

To complete the preparation, the assembled rig was laid horizontal on a wooden cradle and rotated about the heater axis until two of the formers lay vertical and the other horizontal. Four of the five free thermocouples were attached to the outside of the sample container in line with the formers. The fifth was positioned in free air, 300 mm from the rig. Once prepared, each sample was left for 14 days to come to thermal and moisture equilibrium.

To start tests in which constant power was supplied to the heater all temperatures were recorded, the laboratory power supply set to a pre-determined voltage, and a clock started. All temperatures were then read at intervals. For tests in which the heater temperature

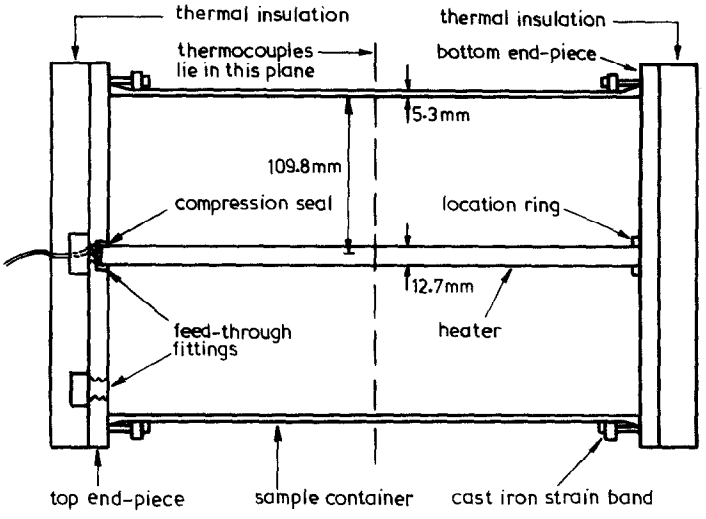

FIG. 1. The sample container with the end-pieces and heater in position.

Table 2. Initial condition of the samples

Sample No.	Moisture content by volume	Heating power ($W\ m^{-1}$)	Heater temperature (°C)
1	0.023	53.8	—
2	0.023	20.0	—
3	0.048	96.0	—
4	0.023	—	60.0

Table 3. Heating powers and duration of tests on sample 2

Heating power ($W\ m^{-1}$)	Duration of test (days)
20.0	13
30.0	10
40.0	12
53.8	14

was to be kept constant the same procedure was followed but with a relay inserted in the electric circuit between the power supply and the heater. This relay was switched on and off under computer control to maintain the heater temperature (which was sensed via a thermistor fixed to the surface of the heater and interfaced to the computer) within a narrow range. An automatic record was made of the proportion of time the relay was closed over 15 min intervals and from this the instantaneous average heating power was estimated. A running sum of the proportions was also kept and saved as a record of the integral of power supplied over time.

RESULTS AND DISCUSSION

In the field, moisture contents at or below the field capacity (~ 0.05 by volume) are expected so only moisture contents in this range were considered. The initial condition of the four samples tested are given in Table 2. Samples 1–3 were heated at constant power. Sample 1 was heated for 28 days and sample 2 for 13 days; at these times increases in temperature were no longer being recorded. Heating was continued for sample 2 for the periods and at the heating powers given in Table 3. By this approach the steady temperature within sample 2 was recorded for a range of heating powers. Sample 3 was heated for only 9 h as an over-temperature safety device was triggered and the power supply switched off. Sample 4 was heated with the heater at constant temperature (60 ± 0.9°C).

On analysing the temperature data recorded for the air surrounding the rig it was found that there was a 95% probability that it was in the range 20.9 ± 1.5°C at any time. Readings taken simultaneously for the four thermocouples attached to the outside of the sample container showed a systematic variation of up to 1 K. This is thought to have been caused by the non-uniform distribution of air from the room air-conditioning unit.

The data recorded for the groups of eight thermocouples attached to the three formers were analysed to see if two-dimensional heating effects could be detected. No such effects were detected; the maximum instantaneous temperature difference recorded between positions at the same radius from the centre of the heater, but on different radials, was 1.3 K. This difference is explained fully by the ± 0.2 K precision of measurement compounded with the 1 K systematic variation measured around the sample container.

The random fluctuations of ± 1.5 K in room air temperature are transmitted to the sample and are superimposed on its thermal response as waves slowly moving radially. Both these fluctuations and the ± 0.2 K precision for temperature measurement must be allowed for when comparing temperatures recorded at the same time but for different radii. By the theory

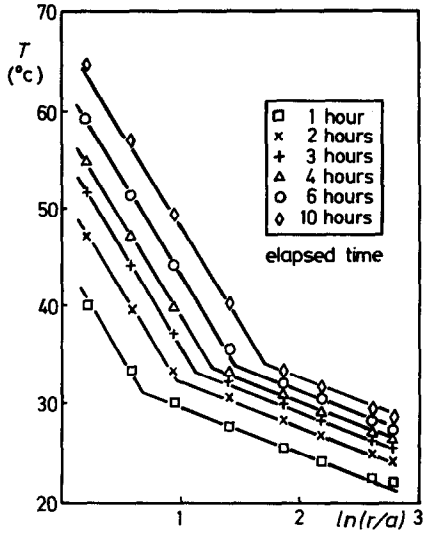

FIG. 2. Temperature in sample 1 during the early stages of heating.

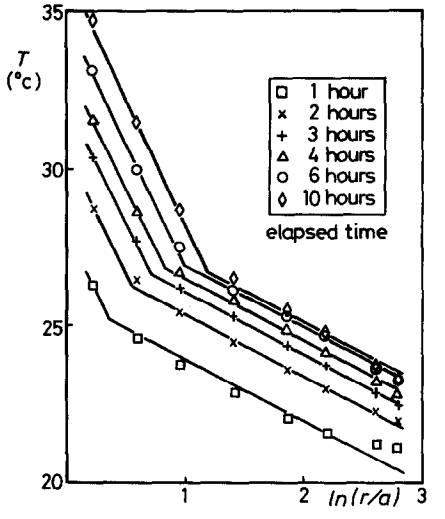

FIG. 3. Temperature in sample 2 during the early stages of heating.

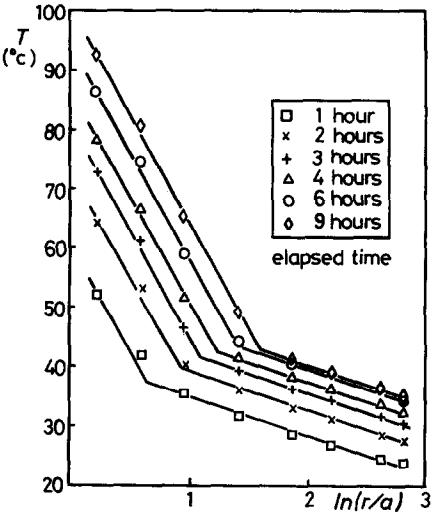

FIG. 4. Temperature in sample 3.

of propagation of errors (for a discussion of this and other statistical theories see Chatfield [8]) the compound inaccuracy from these sources is ± 1.5 K, that is $\pm\sqrt{(1.5^2+0.2^2)}$. For the comparison of temperatures recorded at the same radii but in different samples only the ± 1.5 K room air temperature fluctuation must be allowed for. For convenience, since the accuracy for both cases is ± 1.5 K, it will be described under the general term experimental accuracy.

From Tables 2 and 3 it can be seen that steady temperatures were recorded for both samples 1 and 2 on heating at 53.8 W m^{-1}. These data were analysed to check for repeatability; the average difference between the two sets of data is 0.6 K which represents only 2% of the average difference in temperature between the sample and the air surrounding the experimental rig. The explicable average difference between two sets of eight data each with an accuracy of ± 1.5 K is ± 0.75 K, that is $\pm\sqrt{(2\times 1.5^2/8)}$. The 0.6 K difference quoted above is within these limits so there is no statistically significant difference between the steady temperatures recorded on independently heating samples 1 and 2 with the same heating power; the heating experiments are—at least in this one case—repeatable.

A representative selection of temperature data collected over the first 10 h of heating samples 1–4 are plotted in Figs. 2–5. The steady temperatures recorded for sample 2 are plotted in Fig. 6. At the final heater setting (53.8 W m^{-1}) the moisture distribution along a horizontal radial in sample 2 was examined. The bottom end-piece was removed and half the sample dug out. Large sub-samples were then removed, weighed, dried in an oven at 110°C for 24 h, and then re-weighed. The resulting figures for the moisture distribution are given in Table 4.

There is evidence that non-radial moisture flow under gravity took place within the sample. The moist region corresponding to the final entry in Table 4 was thicker near the bottom of the sample; on visual inspection it extended 23 mm (between radii of 87 and 109.8 mm) compared to 16 mm along the horizontal radial. Also, the full initial moisture charge is not contained in a sample with the radial moisture distribution given in Table 4. As the glass sample container is water and vapour tight this indicates that the moisture content near the bottom of the sample is high; calculations show it must be greater than the field capacity (given earlier as ~0.05 by volume). As will be shown later, a moist region is a distinct feature from the early stages of heating. The region narrows slowly with time until, after many days, its width is thin but steady. Most of the moisture charge is contained in this region so, as it narrows, its volumetric moisture content rises. It is likely, therefore, that gravitational flow is not initiated until the late

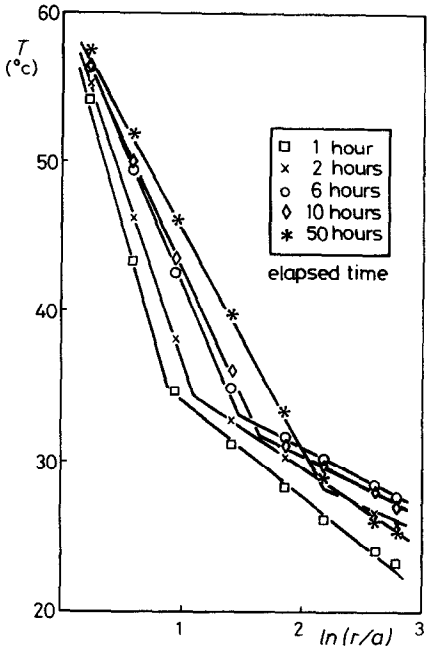

FIG. 5. Temperature in sample 4 during the first 50 h of heating.

Table 4. Final distribution of moisture along a horizontal radial in sample 2

Radii (mm)	Moisture content by volume
6.35/30	0.0009
30/50	0.0014
50/65	0.0018
65/80	0.0020
80/94	0.0037
94/109.8	0.045

stages of heating (long after the temperature data used in the development of the empirical model is collected) when the moisture content finally reaches the field capacity. As noted earlier, non-radial temperature effects were not detected; this indicates that the influence of gravitational moisture flow on temperature response is small even during the very late stages of heating.

Empirical model for heating at constant power

The temperature plots in Figs. 2–4 are (within the natural scatter of the data) piecewise-linear in the natural logarithm of radius with gradients independent of time. According to equation (1), a linear temperature response indicates that the radial heat flux and the local effective thermal conductivity are constants or at least are proportional to one another. Assuming they are constant, the plots in Figs. 2–4 indicate that when heated at constant power the thermal response of the sand is quasi-steady (the heat flux is independent of radius) in two regions each with a uniform effective thermal conductivity which does not vary with time. It is assumed that the junctions of the

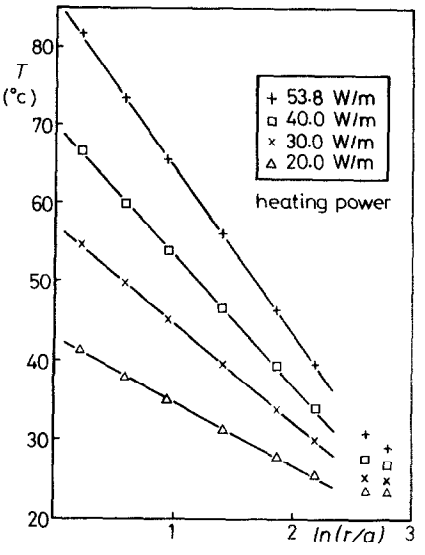

FIG. 6. Steady temperature in sample 2.

linear curves indicate the position of a dry/moist front which separates the dry region around the heater from a moist region. The constant effective thermal conductivities in these regions are called the dry and moist region effective thermal conductivities.

On plotting the values picked by eye from plots of all the temperature data collected it was found that, to a very good approximation, the radius of the dry/moist front (s) moves out with time as follows:

$$s^2 = a^2 + Dt \tag{2}$$

where a is the radius of the heater and D a different constant for each experiment. By definition the constant D has the dimensions of a diffusivity—length^2/time—so is called the drying diffusivity. This form for the rate of progress of the dry/moist front is in agreement with the recent theoretical predictions (based on numerical modelling of combined heat and mass transfer in a silty sand) of Couvillion and Hartley [7].

Best estimates were sought for the three parameters introduced above: the dry and moist region effective thermal conductivities (k_d and k_m) and the drying diffusivity. A non-linear downhill simplex minimization routine [9] was set up to find the values of the parameters that lead to a minimum in the sum of squares of errors between the measured temperatures and those predicted by an empirical model.

The empirical model is simply a statement of the sum of the observations made above. On introduction of length scale, Z, such that

$$Z = \ln(r/a) \tag{3}$$

and on manipulation of equation (1), the empirical model may be written in mathematical terms as

$$W(Z,t) = \begin{cases} f(t) - \Lambda\Gamma Z, & Z \leqslant Z' \\ f(t) - \Lambda\Gamma Z' - \Lambda(Z - Z'), & Z > Z' \end{cases} \tag{4}$$

Table 5. The 95% confidence intervals for the parameters and the error of prediction of the empirical model for heating at constant power

Sample No.	Number of data	k_d (W m^{-1} K^{-1})	k_m (W m^{-1} K^{-1})	$D \times 10^8$ (m^2 s^{-1})	Error (K)
1	128	0.42±1%	1.82±3%	3.23±3%	±0.6
2	144	0.41±2%	1.63±2%	1.16±5%	±0.3
3	128	0.42±1%	2.27±4%	2.94±4%	±1.3

where the predicted temperature (W) is a piecewise-linear function of the length scale with a break point at the position of the dry/moist front (Z'). From equations (2) and (3)

$$Z' = 0.5 \ln (1 + Dt/a^2). \quad (5)$$

The parameters identified from the minimization procedure are D, Γ and Λ where

$$\Gamma = k_m/k_d \quad (6)$$

and

$$\Lambda = Q/(2\pi k_m) \quad (7)$$

and Q is the power per unit length supplied to the heater.

The function f in equation (4) is an arbitrary function of time; it allows the absolute temperature predictions to float, thus eliminating (from the identification of the best parameter values) the influence of the free floating outer boundary condition.

At very early times the thermal responses are not quasi-steady; the temperature plots are curved showing the transient response of the sample to the newly applied heating power. As it is the long-term quasi-steady response which is of interest, data collected during the first hour of heating were not used in the identification of the best parameter values. Neither were data collected after 10 h of heating: the glass sample container provides an impermeable barrier and it is suspected that the influence of this on the rate of drying will build up with time masking the natural drying behaviour that would be seen in the field. The 95% confidence interval for the identified parameter values and the errors of prediction of temperature are given in Table 5. The errors can be seen to be within the experimental accuracy (±1.5 K). No refinement of the empirical model is therefore justified: it contains the minimum information needed to describe the main features seen on visual inspection of the temperature plots and passes the strictest practical statistical test. Lines are drawn through the predictions of the empirical model in Figs. 2–4.

On inspecting Fig. 6 it can be seen that, under steady conditions (within the natural scatter of the data), the gradients of temperature are constant over large regions adjacent to the heater. Best estimates for the effective thermal conductivities in these dry regions were determined using simple linear regression; the resulting values are given in Table 6 and the best lines are drawn in Fig. 6. There are insufficient data to draw any conclusions about the effective thermal conductivity in the moist regions.

Table 6. The effective thermal conductivity within the dry region in sample 2 under steady conditions

Heating power (W m^{-1})	k_d (W m^{-1} K^{-1})	95% confidence interval (%)
20.0	0.39	5
30.0	0.38	3
40.0	0.39	3
53.8	0.40	2

Empirical model for heating at constant temperature

Studying Fig. 5 it can be seen that (within the natural scatter of the data) the temperature plots for the sample heated at constant temperature are piecewise-linear suggesting the thermal response for this type of heating is also quasi-steady. What is not clear from Fig. 5 is whether the effective thermal conductivities in the dry and moist regions are constants, independent of time.

On plotting values picked by eye from plots of all the data collected it was found that the radius of the dry/moist front is approximately given by

$$s^2 = \alpha a^2 + Dt \quad (8)$$

where α is approximately 5. A better fit to the data was sought. As the front must start at the surface of the heater, $s = a$ at $t = 0$. Equation (8) therefore suggests that the front moves off very quickly and then settles down to the behaviour seen in constant heating power tests. There is a parallel to this in the power supplied to the heater during the heating of sample 4: the heating power was initially very high (averaging 146.8 W m^{-1} over the first 15 min) and then settled down to a modest level (52.5 W m^{-1} after 3 h and 41.6 W m^{-1} after 10 h). This suggests an equation for the progress of the dry/moist front of the form

$$s^2 = a^2 + \hat{D}h(Q)t. \quad (9)$$

The most obvious equations are

$$s^2 = a^2 + \hat{D}Qt \quad (10)$$

and

Table 7. The 95% confidence intervals for the parameters and the error of prediction of the empirical model for heating at constant temperature

Sample No.	Number of data	k_d (W m^{-1} K^{-1})	k_m (W m^{-1} K^{-1})	$\hat{D}\times 10^{10}$ (m^3 J^{-1})	Error (K)
4	128	$0.39\pm1\%$	$1.71\pm2\%$	$5.6\pm2\%$	±0.4

$$s^2 = a^2 + \hat{D}\int_0^t Q\,dt. \tag{11}$$

These were tested against the experimental data and equation (11) found to be very good: better than equations (10) and (8).

From the observations above an empirical model can be set up for the thermal response of the sand when heated at constant temperature. On the assumption that the effective thermal conductivities in the dry and moist regions are constant, the response can again be described by equation (4), but with

$$Z = Q\ln(r/a) \tag{12}$$

$$\Lambda = 1/(2\pi k_m) \tag{13}$$

and

$$Z' = 0.5Q\ln\left(1+\frac{\hat{D}}{a^2}\int_0^t Q\,dt\right). \tag{14}$$

The best values identified for parameters k_d, k_m and $\hat{D}$ are given in Table 7 along with the error of prediction of the empirical model. At ±0.4 K the error is well within the experimental accuracy (±1.5 K). This suggests that the empirical model is good, the effective thermal conductivities in the dry and moist regions are constants and the progress of the dry/moist front is well described by equation (11).

Lines are drawn through the predictions of the empirical model in Fig. 5. For interest, the experimental temperature data collected after 50 h of heating have been plotted in the figure along with lines drawn through the empirical model predictions extrapolated to this time. The temperatures are quite well predicted: all discrepancies are within the ±1.5 K experimental accuracy. The empirical model therefore appears to be accurate well beyond the 10 h heating time for which it has been validated.

Interpreting the empirical model

Adams and Baljet [1] established that a distinct dry region is created when unsaturated uniform sand is heated. What has been shown here is that during drying both the dry and moist regions have essentially constant effective thermal conductivities and the rate of progress of the dry/moist front at the boundary of the two regions can be expressed in a simple analytic form.

The term effective thermal conductivity is used here as the ratio of total heat flux to the macroscopic temperature gradient. In practice, as discussed by de Vries [10], the total heat flux in moist soils comprises contributions from thermal conduction through the soil solids and fluids, sensible (convective) heat flow in the soil fluids, and latent heat flow in the vapour phase of soil water. It is known [11] that the effective thermal conductivity of the sand is very sensitive to moisture content, and (through the influence of temperature on soil water vapour density, as described by de Vries [12]) is very sensitive to temperature, especially at temperatures above 50°C.

Studying Table 4 it can be seen that the moisture content in dry regions is very low and varies little with radius. As the effective thermal conductivity has been shown to be constant this variation in moisture content must be so small as to induce insignificant radial variations in effective thermal conductivity. The temperature plots show that the temperature in dry regions is high and varies greatly with radius. The effective thermal conductivity in dry regions must therefore be insensitive to large variations in temperature. This may be explained only if there is little or no latent heat flow; the moisture content in dry regions must therefore be so low that significant soil water vapour density cannot be sustained.

The temperature plots show that all the moist regions are at low temperature. As the variations in temperature with radius are also small (typically the differences across the moist regions are less than 10 K) significant temperature induced radial variations in effective thermal conductivity are not to be expected. The moisture content in the moist regions is not known. As the effective thermal conductivities have been found to be uniform this suggests that there is little radial variation in moisture content within moist regions. If this view is correct, the moisture profile in the sand is well described by a two-level model: the moisture content is very low in the dry region and steps up to a high value at the dry/moist front; it maintains this high value right to the outer boundary of the sample.

Some conclusions can be drawn from the form of the analytic expression for the rate of progress of the dry/moist front. Assuming the two-level moisture model, the rate at which water must move with the dry/moist front is given by

$$q = 2\pi\rho M s\frac{ds}{dt} \tag{15}$$

where q is the mass flow rate per unit length of heater and ρ and M are the liquid soil water density (10^3 kg m^{-3}) and the volumetric moisture content in the moist region. On differentiating the empirical equation for

Table 8. Values for the ratio Lq/Q calculated using equation (18)

Sample No.	Lq/Q
1	0.104
2	0.101
3	0.111
4	0.097

the radius of the dry/moist front (equation (11)) and substituting into equation (15)

$$q = \pi\rho M\hat{D}Q \tag{16}$$

where, for heating at constant power

$$\hat{D} = D/Q. \tag{17}$$

Equation (16) shows that, ignoring the slight increase in the moist region moisture content with time, the instantaneous net rate of mass flow at the dry/moist front is directly proportional to the instantaneous heating power.

A comparison can now be made of the rate of mass flow in the four experiments. This can be achieved using the non-dimensional ratio Lq/Q where L is the latent heat of vaporization of soil water (taken here as 2.4×10^6 J kg^{-1}). From equation (16), the ratio is given by

$$\frac{Lq}{Q} = \pi\rho LM\hat{D}. \tag{18}$$

It represents the ratio of the instantaneous power required to evaporate the net mass of water flowing with the dry/moist front to the instantaneous heating power. The ratio was calculated for the four experiments assuming the moisture content in the moist region is well approximated by the initial sample moisture content; the resulting values are listed in Table 8. All four figures lie in the narrow range $0.104 \pm 7\%$ suggesting an equation of the form

$$\frac{Lq}{Q} = 0.1 \tag{19}$$

may be applicable over a large range of temperature, heating power and moisture content.

CONCLUSIONS

Even under moderate heating loads uniform medium sand with a moisture content below the field capacity is thermally unstable. When the sand is heated by a buried cylinder a dry region with very low moisture content develops around the heater and grows with time. The transient thermal response of the sand is much quicker than its moisture response; the thermal response soon settles down to being quasi-steady with heating power flux independent of radius.

Whether the heater is supplied with constant power or is maintained at constant temperature, the effective thermal conductivities in the dry and moist regions of the heated samples are independent of both time and radius; the typical dry region effective thermal conductivity for the high quartz sand tested is 0.4 W m^{-1} K^{-1} while that in moist regions is typically 4.5 times as large.

Taking the very distinct knees in plots of temperature data recorded during heating to coincide with a distinct dry/moist front at the boundary of the dry and moist sand, the progress of the front was found to be well described by

$$s^2 = a^2 + \hat{D}\int_0^t Q\,\mathrm{d}t \tag{20}$$

where s and a are the radii of the front and at the heater, Q the instantaneous heating power at time t, and $\hat{D}$ a drying constant (different for each initial sample moisture content and heater power or temperature tested). It was also found that, for the range of experimental conditions tested

$$\frac{Lq}{Q} = 0.1 \tag{21}$$

where L is the latent heat of vaporization of soil water and q the net rate of water mass flow at the dry/moist front.

From the observations recorded above it was concluded that the moisture content in the dry region is so low as to be unable to sustain significant water vapour density. The moisture content rises very steeply to a high value at the dry/moist front and then varies little across the moist region.

The uncomplicated nature of the sand's thermal response may be exploited in several ways. For example, in determining the long-term thermal insulation properties of the sand, in the development of a numerical model for thermal instability in regions with complex geometry, and in characterizing and comparing the thermal insulating properties of different soils.

Acknowledgements—This work was sponsored by the Science and Engineering Research council under grants GR/C/35646 and GR/D/69976. I gratefully acknowledge this support and the helpful advice offered by the grantholders, Professor B. J. Brinkworth, Head of the Department of Mechanical Engineering and Energy Studies, and Dr H. R Thomas, Lecturer in the Department of Civil and Structural Engineering.

REFERENCES

1. J. I. Adams and A. F. Baljet, The thermal behavior of cable backfill materials, *IEEE Trans. Pwr Apparatus Systems* **PAS-87**, 1149–1161 (1968).
2. J. Ewen, Combined heat and mass transfer in unsaturated sand surrounding a heated cylinder, Ph.D. thesis, University of Wales (1987).
3. W. O. Smith, Thermal transfer of moisture in soils, *Trans. Am. Geophys. Un.* **24**, 511–523 (1943).

4. J. Y. Baladi, D. L. Ayers and R. J. Schoenhals, Transient heat and mass transfer in soils, *Int. J. Heat Mass Transfer* **24,** 449–458 (1981).
5. R. L. Rollins, M. G. Spangler and D. Kirkham, Movement of soil moisture under a thermal gradient, *Highway Res. Board Proc.* **33,** 492–508 (1954).
6. D. J. Shah, J. W. Ramsey and M. Wang. An experimental investigation of the heat and mass transfer coefficients in moist, unsaturated soils, *Int. J. Heat Mass Transfer* **27,** 1075–1085 (1984).
7. R. J. Couvillion and J. G. Hartley, Drying front movement near low-intensity, impermeable underground heat sources, *Trans. ASME J. Heat Transfer* **108,** 182–189 (1986).
8. C. Chatfield, *Statistics for Technology*, 3rd Edn, p. 206. Chapman & Hall, London (1983).
9. W. H. Press, B. P. Flannery, S. A. Teukolsky and W. T. Vetterling, *Numerical Recipes*, p. 289. Cambridge University Press, Cambridge (1986).
10. D. A. de Vries, The theory of heat and moisture transfer in porous media revisited, *Int. J. Heat Mass Transfer* **30,** 1343–1350 (1987).
11. J. Ewen and H. R. Thomas, The thermal probe—a new method and its use on an unsaturated sand, *Geotechnique* **37,** 91–105 (1987).
12. D. A. de Vries, Heat transfer in soils. In *Heat and Mass Transfer in the Biosphere*, 1. *Transfer Processes in the Plant Environment* (Edited by D. A. de Vries and N. H. Afgan), pp. 5–28. Scripta, Washington, DC (1975).

APPENDIX

The following equations for the capillary potential, the unsaturated hydraulic conductivity, and the thermal conductivity of Garside Grade 21 sand at 20°C have been drawn from ref. [2]. These equations are not used in the development of the empirical model.

Capillary potential (ψ) was determined using volumetric pressure plate extraction equipment. For a sample compacted to a dry density of 1650 kg m^{-3}

$$\psi/g = (-0.25 - 1.06 \times 10^{-3} S^{-1.75}) \pm 6\% \text{ m} \quad (0.013 \leqslant S < 1) \tag{A1}$$

where g is the gravitational constant (9.81 m s^{-2}) and S the degree of saturation defined as the ratio of the volume occupied by soil water to that occupied by soil water and moist air.

Unsaturated hydraulic conductivity (K) was determined using horizontal infiltration equipment. For a sample compacted to a dry density of 1700 kg m^{-3}

$$gK = 1.5 \times 10^{-10 \pm 1.13} \exp(28.061S - 12.235S^2) \text{ m s}^{-1} \quad (0.133 < S \leqslant 1). \tag{A2}$$

Thermal conductivity (k) was determined using a line source thermal probe. After adjusting collected data to a common dry density of 1580 kg m^{-3}

$$k = (0.34 + 2.07(1 - \exp(-8.9S))) \pm 7\% \text{ W m}^{-1}\text{K}^{-1} \quad (0 \leqslant S \leqslant 1). \tag{A3}$$

INSTABILITE THERMIQUE DANS UN SABLE INSATURE FAIBLEMENT CHAUFFE

Résumé—Des échantillons de sable insaturés sont chauffés à quelques dizaines de Kelvin par un petit chauffoir électrique. Les profils radiaux de température présentés montrent clairement une instabilité lorsqu'une région sèche se développe autour du chauffoir. On développe un modèle empirique simple et général, à trois paramètres constants. Deux d'entre eux sont les conductivités thermiques effectives dans le sable sec et humide tandis que le troisième est lié au taux de séchage.

THERMISCHE INSTABILITÄT IN MÄSSIG BEHEIZTEM, UNGESÄTTIGTEM SAND

Zusammenfassung—Proben ungesättigten Sands wurden mit einem kleinen zylindrischen Heizelement einige zehn Kelvin aufgeheizt. Die hier präsentierten radialen Temperaturprofile zeigen deutlich Instabilitäten, sobald das Gebiet um das Heizelement austrocknet. Es wurde ein einfaches, allgemein nützliches, empirisches Modell mit drei konstanten Parametern entwickelt. Zwei der Parameter sind die effektiven Wärmeleitfähigkeiten in trockenem und feuchtem Sand, während sich der dritte auf die Trocknungsgeschwindigkeit bezieht.

ТЕПЛОВАЯ НЕУСТОЙЧИВОСТЬ ВО ВЛАЖНОМ ПЕСКЕ ПРИ СЛАБОМ НАГРЕВЕ

Аннотация—От небольшого цилиндрического источника на несколько десятков градусов Кельвина нагревались образцы влажного песка. Приведенные в статье радиальные профили температуры дают четкое представление о возникновении неустойчивости по мере высыхания жидкости вокруг нагревателя. Разработана простая и удобная эмпирическая модель с тремя постоянными параметрами, два из которых—эффективные коэффициенты теплопроводности сухого и влажного песка, а третий связан со скоростью сушки.